THE ASTROPHYSICAL JOURNAL, 310:1–18, 1986 November 1

LARGE-SCALE CLUSTERING OF GALAXIES WITH MASSIVE DARK HALOS. I. GENERAL STRUCTURE, TWO-POINT CORRELATIONS, AND BINARIES

AUGUST E. EVRARD
Physics Department, State University of New York at Stony Brook, and Institute of Astronomy, University of Cambridge
Received 1986 February 21; accepted 1986 April 16

ABSTRACT

N-body simulations of large-scale clustering of galaxies with massive dark halos are performed and compared to models where galaxies are treated as point masses. Simulations with 800 galaxies in both a flat ($\Omega = 1.0$) and open ($\Omega_f = 0.15$) universe are evolved from a Poisson initial density distribution in a periodic comoving cube of final length 63 Mpc. In the dark matter models, two "species" of particles are used, galactic systems are comprised initially of a single "luminous" particle centered in an extended halo of 25 "dark" particles following a truncated isothermal profile $\rho \propto r^{-2}$. Ninety percent of the total mass is contained in the halos, which are not "locked" to a given galaxy, but are subject to disruption, stripping, and merging in a self-consistent fashion.

The extended halos smooth the mass distribution and introduce significant inelasticity into galaxy encounters which is nonexistent in models where galaxies are modeled as softened point masses. Dynamical friction increases the galactic density at the centers of groups and clusters and enhances the two-point correlation function $\xi(r)$ on small scales, but the clustering on 5–10 Mpc scales is suppressed relative to the point mass case. Peculiar velocities of galaxy pairs are reduced significantly—agreement with observations is found for the $\Omega_f = 0.15$ model on scales $1 \leq H_0 r/\mathrm{km\ s^{-1}} \leq 100$, but the $\Omega = 1.0$ model velocities remain too high. The distribution of isolated binaries in the open model becomes bimodal: those pairs of galaxies inside merged common halos contract because of dynamical friction, while those unbound at larger separations recede in the general expansion leaving a "hole" between 80 kpc and 1.0 Mpc where almost no binaries are found. In both models, binary velocities are reasonably flat functions of separation, in agreement with observed behavior and in contrast to the point mass models which show Keplerian falloff.

Both models require an initial density distribution with more power on large scales to match the observed power-law behavior of $\xi(r)$. The low-density model suffers from too much dynamical friction which may be alleviated by reducing the amount of dark mass in halos or by beginning from a more recent epoch. It is argued that the $\Omega = 1.0$ model will require some biasing of the galaxy distribution to reduce the amount of mass in the local vicinity of galaxies. Such a mechanism may be necessary for lowering small-scale peculiar velocities to observational values in a critically dense universe.

Subject headings: cosmology — galaxies: clustering — galaxies: structure — numerical methods

I. INTRODUCTION

Our present understanding of the dynamics of matter on galactic and larger scales indicates that a substantial amount of mass exists outside the visible regions of galaxies. Flat rotation curves of H I in edge-on spiral galaxies (Van Albada *et al.* 1985) provide perhaps the best evidence for the existence of dark matter surrounding galaxies. Fits to the velocity profiles using multicomponent mass models (Bahcall and Casertano 1985) evidence the dark matter to be distributed in a roughly isothermal fashion, $\rho \propto r^{-2}$, with interior mass ratio $M_{\mathrm{dark}}/M_{\mathrm{lum}} \approx 1$ at the Holmberg radius. At larger distances, the independence of isolated binary galaxies' velocity with separation (Ostriker, Peebles, and Yahil 1974; Einasto, Kaasik, and Saar 1974) suggests this isotherml distribution extends out to nearly megaparsec scales, although quantitative analysis is difficult for binaries (White *et al.* 1983; Sharp 1984). X-ray studies of gas in clusters of galaxies and around individual massive galaxies (Fabricant and Gorenstein 1984; Stewart *et al.* 1984) also require dominant amounts of unseen mass to satisfy hydrostatic equilibrium. In the case of M87, the total mass increases roughly linearly with radius reaching $M_{\mathrm{tot}} \approx 10^{13}\ M_\odot$ at $r \approx 100$ kpc, almost two orders of magnitude greater than the system's luminous mass of $\sim 2 \times 10^{11}\ M_\odot$. Finally, virial mass estimates of galaxy groups (Geller and Huchra 1983; Heisler, Tremaine, and Bahcall 1985) and clusters (Faber and Gallagher 1979) consistently give mass-to-light ratios 100 times or more larger than typical stellar values. Again, it has not been possible to model the dark matter distribution in detail on these scales, although attempts have been made for well-observed rich clusters such as Coma (Des Forêts *et al.* 1984). The general indication is that on the largest clustered scales, a dominant fraction (fiducial value 90%) of the total mass may not be visible.

Given that a substantial amount of dark material exists distributed well outside the luminous parts of galaxies, it is only natural to ask how this mass will affect the development of structure in the galaxy distribution. Since the pioneering work of Holmberg (1941), direct simulations have shown that encounters between extended massive systems are highly inelastic (see reviews by Tremaine 1981; White 1983; Alladin and Narasimhan 1983). Orbital energy of the systems' bulk motions is spent in disrupting their individual halos to produce a common envelope, if bound. The time scale for this process is quite rapid, usually comparable to the characteristic dynamical time scale—crossing time for a group or orbital period for a binary. White (1978) realized that interactions between

extended unseen halos around galaxies would have serious effects on the *majority* of galaxy encounters. Such a situation could arise if galaxies formed within extended dark envelopes, as in, for example, a two-stage process suggested by White and Rees (1978). As clustering progresses, the *dissipational* character of halo interactions will provide an important energy "sink" which will appreciably affect the kinematic properties of the galaxies.

The only tractable way to realistically model the nonlinear evolution of clustering on a large scale is through N-body simulation. This paper reports results of simulations in which two "species" of particles are used; the luminous mass in a galaxy is represented by a single "luminous" particle which is initially centered in an isothermal-profile halo represented by 25 "dark" particles. Ninety percent of the total mass is assumed to be in the dark component. At the start of the calculations, 800 such galactic systems (20,800 total particles) are distributed randomly in a periodic cube of final length 63 Mpc on a side. Models were evolved within a flat ($\Omega = 1.0$) and open ($\Omega_f = 0.15$) universe.

Due partly to numerical limitations, previous cosmological simulations (Gott, Turner, and Aarseth 1979; Efstathiou and Eastwood 1981; Davis *et al.* 1985) assumed a one-to-one correspondence between galaxies and particles in the simulation; i.e., each galaxy is represented by a single particle of mass m and "size" $\epsilon/(2)^{1/2}$. The softening parameter ϵ reduces the gravitational force at small separations through use of the Plummer potential $\Phi(r) = -Gm^2/(r^2 + \epsilon^2)^{1/2}$. Inherent in this representation are assumptions that (1) galaxies *identically* trace mass and (2) galaxies interact *elastically*. Both of these assumptions are suspect in light of the inferred existence of extended dark halos around galaxies and the knowledge of the inelastic character of their encounters. Prior models have been successful in reproducing properties of the observed density distribution such as the two-point, $\xi(r)$, and three-point, $\zeta(r)$, galaxy correlation functions for $\xi(r) \leq 10^3$. The two-point correlation function has been observed to retain its power-law shape down to scales of a few tens of kpc where $\xi(r) \approx 10^5$ (Gott and Turner 1979). It is not known what effect the addition of massive halos of size about a few hundred kpc will have on small-scale clustering properties. Another problem in previous large-scale models has been their inability to reproduce the peculair velocity profile $\sigma(r)$ of random galaxy pairs. Peculiar velocities generated on clustered scales have been uncomfortably large, particularly in high-density models where one-dimensional velocity dispersions $\sigma \approx 1000$ km s^{-1} are not uncommon (see, e.g., Davis *et al.* 1985). Observational values of σ fall between ~ 100 km s^{-1} and ~ 350 km s^{-1} (Davis and Peebles 1983; Bean *et al.* 1983; Rivolo and Yahil 1981). Also, models employing single particle galaxies have been unable to reproduce the kinematic properties of isolated binary galaxies (Evrard and Yahil 1985). The highly concentrated mass distribution for individual galaxies leads to velocities falling in a Keplerian fashion with pair separation rather than remaining flat as observed. Thus, the full kinematic picture points to the need for some dissipative mechanism to help reduce peculiar velocities on clustered scales and to tend to keep velocities flat as a function of separation.

The two-component approach used here is similar to that used by Barnes (1983, 1984) in simulating the dynamical evolution of small groups of galaxies possessing massive dark halos. His simulations have demonstrated that the inelasticity of halo encounters can significantly alter group kinematics. Groups which appear "old," in terms of their fiducial crossing times being a small fraction of a Hubble time, may actually be dynamically very young objects. One significant point is the fact that, during the evolution of the groups, the galaxies' virial velocity remains roughly constant as their virial radius decreases. The exact cause and universality of this regulatory process are not well understood, but the results are encouraging in view of the flat nature of velocities seen from rotation curves around galaxies out to velocities of random galaxy pairs at a few Mpc.

The focus in this paper is on exhibiting the effects of dark matter on observable properties of the galaxy[1] distribution. This is important in relating the input physics of the models to the real world. The full dynamical picture can be understood only by examining the relative distributions of dark and luminous matter. The next paper in this series (Evrard 1986) will focus on the distribution of dark matter on a variety of scales—from individual galaxies to binaries to clusters of galaxies. Topics to be considered will be the existence of flat rotation curves around galaxies, systematic effects on dynamical mass estimates, and trends in "mass-to-light" ratios on scales from individual galaxies to clusters containing ~ 50 galaxies.

A detailed explanation of the models, including initial conditions, is given in § II. In § III, results from the runs including dark matter halos around galaxies are compared with runs in which galaxies are represented as softened point masses. Differences are evident from visual inspection and from measurement of the galaxy two-point positional and velocity correlations. Isolated binaries are useful in probing the realism of the small-scale dynamics in the models. Comparison of data from both galaxy "representations" with observations sheds light on the improvements made by the inclusion of dark matter halos around galaxies. These points and hopes for even more realistic treatments are discussed in the final section.

II. THE MODELS

The results of four simulations are reported in this paper, two each for $\Omega = 1.0$ and $\Omega_f = 0.15$. For each background cosmology, one run with dark matter halos around galaxies (labeled DM) and one using single particle (SP) galaxies were performed. The initial spatial distribution of the galaxies is the same in all four runs—random positions were assigned within a cubic simulation volume. This facilitates direct comparison of structure between the models. Clustering evolved from such "white noise" initial power spectra in previous studies (Gott, Turner, and Aarseth 1979; Efstathiou and Eastwood 1981) has generally not been able to match observed clustering, as measured by the two-point correlation function $\xi(r)$. Thus, from the outset, we do not expect to produce a good match to $\xi(r)$ over a wide range of scales. Since $\xi(r)$ is usually employed as the "meter stick" to signal when to stop a calculation, we must use another criteria for determining what epoch in the models to match with observations. A simple theoretical procedure is outlined below.

The spirit motivating the set of models presented in this paper is one of trying to get a feel for the effects introduced by galactic halos into the dynamics of the clustering process, as measured by global statistical properties such as $\xi(r)$ and $\sigma(r)$. The principal advantage of using a white noise intitial spec-

[1] Unless noted otherwise, the term *galaxy* refers to luminous matter only. Thus, "galaxy distribution" refers to the distribution of luminous particles in the simulations, "galaxy pairs" refers to pairs of luminous particles, and so on.

trum is the fact that it eliminates the need for producing an ensemble of runs for a particular model. As each run consumes ~ 100 hr of CPU on a VAX 11/780, this results in substantial cost savings. Models using initial spectra which evolve to match well the observed $\xi(r)$, for example neutrino or cold dark matter spectra, have significant power on scales comparable to the simulation volume which necessitates the use of several realizations to reasonably sample the large-scale spectrum and provide good statistics. Guided by the results of the white noise models, the two-species approach may then be used in concert with a more "realistic" initial spectrum in a way which will optimize the chances of producing a model which matches the full kinematic and structural properties of the universe over a wide range of scales.

a) Description

The initial density structure in the DM models consists of 800 identical galactic systems, each comprised of a central luminous particle surrounded by a halo of 25 dark particles. The choices of the number of systems and particles per system result from constraints on two opposing sides. To represent a reasonably large volume of the universe requires the simulation contain $\sim 10^3$ galaxies, but the numerical scheme used can comfortably handle only $\sim 3 \times 10^5$ total particles. This leaves a few tens of particles per galactic system. One luminous particle is used per galaxy for simplicity and because there is simply not enough dynamic range to construct a stable bound system of luminous particles within the halo.

The halos themselves are characterized by a rotation velocity $v_{\rm rot}$ and a truncation radius r_t. These, through the density profile

$$\rho(r) = \frac{v_{\rm rot}^2}{4\pi G r^2}, \tag{1}$$

fix the halo mass $M_h = G^{-1} v_{\rm rot}^2 r_t$. Note that "rotation velocity" here is used only to characterize the mass contained within a radial shell, $dM = G^{-1} v_{\rm rot}^2\, dr$. It is *not* meant to imply that the halos are initially rotating. Similarly, the use of the term "isothermal" applies only to the form of the initial density run and is not meant to imply that the velocity dispersion is constant throughout the halos initially. The structure of the initial velocity field is discussed at length below.

Observational values of $v_{\rm rot} \approx 200$ km s^{-1} are common (Bahcall and Casertano 1985). To use this information in constructing the *initial* state of the models requires knowledge of the initial redshift z_i (equivalently, the overall expansion factor $R_f = 1 + z_i$) and the use of a procedure to scale the model to physical units. We use the number density of bright galaxies in the Revised Shapley-Ames (RSA) Catalog (Sandage and Tammann 1980) to scale the final configuration of the models. This method was used by Evrard and Yahil (1985) in a study of virialization in the N-body models of Efstathiou and Eastwood (1981) where the number density of galaxies with absolute magnitude brighter than M_* was found to be[2]

$$n(M_*) = 0.0027 E_i(x_*)\ {\rm Mpc}^{-3}$$

where $E_i(x_*)$ is the exponential integral, $x_* = 10^{-0.4(M_* - M_0)}$, and $M_0 = -20.7$ is the characteristic magnitude in the luminosity function (Yahil, Sandage, and Tammann 1980). This number density is a slowly varying function of M_* for M_* roughly a magnitude or more dimmer than M_0. Choosing

[2] $H_0 = 50$ km s^{-1} Mpc^{-1} is assumed throughout this paper.

TABLE 1

SUMMARY OF MODEL CHARACTERISTICS

Ω_f	R_f	r_t[a]	ϵ[b]	$M_{\rm sys}$[c]	$m_{\rm lum}$[c]	$m_{\rm dark}$[c]
1.0.....	5.47	2.1	58	220	22	7.9
0.15.....	11.7	0.32	27	33	3.3	1.2

[a] Unit Mpc.
[b] Unit kpc.
[c] Unit $10^{11}\ M_\odot$.

$M_* = -19$ fixes the number density at $n = 0.0032$ Mpc^{-3} and the mass per galactic system at $M_{\rm sys} = 2.2 \times 10^{13} \Omega_f\ M_\odot$, Ω_f being the value of the density parameter at the final epoch. The number density in the RSA sample agrees well with that determined from the CfA survey by Davis and Huchra (1982). With 800 galaxies in the simulation, this density implies a final length for the edge of the cubical region to be 63 Mpc.

The fraction of mass in dark matter is taken to be 90%. The mass of each luminous particle is thus 1/10 the system mass and the mass of each dark particle is $m_{\rm dark} = 9/25 m_{\rm lum}$ (see Table 1). The ratio $\beta = m_{\rm dark}/m_{\rm lum}$ is important in determining the strength of dynamical friction effects (Barnes 1984) as the two different components struggle to achieve equipartition. The smaller the ratio, the more the dark material behaves like an ideally smooth background medium and the more pronounced is the dynamical friction. Equipartition will be reached when a luminous particle's kinetic energy is released into the medium and the heavy particle lies motionless in the rest frame of the background. When β equals unity, the two species are indistinguishable (all else being equal) and there should be no dynamical friction, equipartition being achieved when the velocity dispersions of the two species match identically.

The amount of expansion necessary for the models is determined from linear theory by assuming that the mass fluctuation scale presently just going nonlinear, $\delta\rho/\rho \approx 1$, in the real universe typically contains ~ 50 galaxies (Davis and Peebles 1983). Since the galactic distribution in the initial models is Poissonian, the amplitude of a typical fluctuation on a scale of 50 galaxies is just $\delta\rho/\rho \approx 1/(50)^{1/2} = 0.14$. (Galaxies and mass are directly correlated on this scale.) Defining $\epsilon = 1 + \delta\rho/\rho$, the growth of a density perturbation at a given mass scale can be written (Yahil 1985)

$$\frac{d \ln \epsilon}{d \ln R} = \frac{-3u}{Hr} = \Omega^{0.6}(\epsilon - 1)\epsilon^{-0.25}, \tag{3}$$

where the last term on the right-hand side includes an empirically derived approximate expression for the peculiar velocity u valid for linear to moderately nonlinear perturbations. Integrating the above equation from $\epsilon = 1.14$ at $R = 1$ to $\epsilon = 2$ gives the final expansion factor $R_f = 5.47$ ($\Omega = 1.0$) and $R_f = 11.7$ ($\Omega_f = 0.15$).

This information can now be fed back into the determination of the halo truncation radius r_t. Assuming 90% of the system mass is in the halo with $v_{\rm rot} = 200$ km s^{-1}, the halo radius is simply $r_t = 0.9 G M_{\rm sys}/v_{\rm rot}^2 \approx 2.1 \Omega_f$ Mpc (see Table 1). The value of r_t at the initial epoch is set by assuming the halo size remains constant in the proper frame. The value of r_t expressed as a fraction of the initial mean intergalactic spacing $d_i = L_i/N_{\rm gal}^{1/3}$ is

$$\frac{r_t}{d_i} = \begin{cases} 1.6, & \Omega = 1.0 \\ 0.6, & \Omega_f = 0.15 \end{cases} \tag{4}$$

The filling factor of the halos is 0.9 in the open model and 17 for the critical case. Thus, the dark matter is centrally concentrated around the luminous centers initially in the $\Omega_f = 0.15$ model, with $\delta\rho/\rho \approx 4$ at the halo half-mass radius. In contrast, the dark material in the $\Omega = 1.0$ simulation is much more smoothly distributed, density contrasts above unity occurring only at radii $r \leq 0.16 r_t$, a region containing typically four dark particles.

The velocity field of the particles in the simulation is initialized by directly measuring the local peculiar acceleration $\boldsymbol{g}_p(\boldsymbol{r})$ and using the linear theory relation (Peebles 1980)

$$\boldsymbol{v}_{p,\mathrm{lin}}(\boldsymbol{r}_i) = \tfrac{2}{3} H^{-1} \Omega^{-0.4} \boldsymbol{g}_p(\boldsymbol{r}_i) \, . \tag{5}$$

The process is performed in two stages, each species treated separately. First, halo center positions are chosen, the dark particles are distributed in the halos, and a luminous particle placed at each center. The luminous peculiar velocities are set by treating halo systems as a unit and summing the acceleration over centers of mass

$$\boldsymbol{g}_{p,\mathrm{com}}(\boldsymbol{r}_i) = \sum_{\substack{\text{halo} \\ \text{centers } j}} \frac{-GM_{\mathrm{sys}} \boldsymbol{r}_{ij}}{(r_{ij}^2 + \hat{\epsilon}^2)^{3/2}} \, , \tag{6}$$

where $\hat{\epsilon} \approx 0.4 r_t$ is a softening comparable to the system size. For the dark particles, the nonlinear correction to the peculiar velocity is included, $\boldsymbol{v}_p = \boldsymbol{v}_{p,\mathrm{lin}} \times (1 + \delta)^{-0.25}$, where δ is the local overdensity. The peculiar acceleration on a dark particle k in a given halo i is found by taking the acceleration of the ith halo, equation (6), and adding to it the contribution from discrete particles within that halo and any *overlapping* halos j, the contribution from the overlapping halos to equation (6) then being subtracted:

$$\boldsymbol{g}_p(\boldsymbol{r}_k) = \boldsymbol{g}_{p,\,\mathrm{com}}(\boldsymbol{r}_i) + \sum_{\substack{\text{halo } i \\ \text{halos } j}} \sum_{\substack{\text{particles} \\ l \text{ in halo}}} \frac{-Gm_l \boldsymbol{r}_{kl}}{(r_{kl}^2 + \epsilon^2)^{3/2}}$$

$$- \sum_{\text{halos } j} \frac{-GM_{\mathrm{sys}} \boldsymbol{r}_{ij}}{(r_{ij}^2 + \hat{\epsilon}^2)^{3/2}} \, , \tag{7}$$

where ϵ is the softening used for individual particles. If the peculiar velocity for dark particle k found by this procedure is too large; specifically, if $|v_p| > (3/2)^{1/2} v_{\mathrm{rot}}$, then the particle is assigned a random velocity drawn from a Gaussian distribution with one-dimensional velocity dispersion $\sigma = v_{\mathrm{rot}}/(2)^{1/2}$. The resulting velocity field is thermal in the inner regions of the halos and infalling at larger radii.

Initial conditions for the single particle galaxy runs are constructed by simply omitting the halos: the initial particle positions and velocities are identical to those of the luminous particles in the dark halo models. The particle mass in this case, however, is now equal to the total system mass, 10 times that of the luminous particles in the dark matter runs.

The models are integrated using the P^3M N-body program (Hockney and Eastwood 1981) adapted for cosmological use by Efstathiou and Eastwood (1981) and generously made available by Dr. Efstathiou and his collaborators. The scheme constructs the force on each particle by combining a large-scale mesh contribution with a small-scale direct summation, resulting in resolution comparable to fully direct methods while allowing much larger particle number (see Efstathiou *et al.* 1985 for a comparative discussion of the P^3M scheme). The particle softening $\epsilon = 0.005L$ initially is the same for both species and is held fixed in proper coordinates, taking on values at the final epoch denoted in Table 1. Note that these values (a few *tens* of kpc) are about an order of magnitude smaller than those used in previous models (Evrard and Yahil 1985; Davis *et al.* 1985), reflecting the increase in resolution of the mass distribution attained in the dark matter models. The simulations are evolved using time as the independent variable, each dark matter model taking $\sim$1000 times steps while consuming roughly 100 CPU hours on a VAX 11/780. Energy is conserved to $\sim$1.2% ($\Omega = 1.0$) and $\sim$0.3% ($\Omega_f = 0.15$), with momenta and angular momenta conserved to much higher accuracy.

III. RESULTS

a) General Structure

An evolutionary sequence of projections onto the x-y plane of a comoving (20 Mpc)^3 region in the simulations is shown in Figure 1. Galaxies (i.e., luminous particles) are plotted as circles, dark matter particles as points. The region contains 34 galaxies initially—eight more than the 26 expected from Poisson statistics—and contains one of the largest structures grown in the models at the final epoch. The larger halo radius in the critical model is apparent at the initial stage—the dark matter appearing almost uniformly distributed—and the subsequent evolution shows that a fair fraction of dark material remains in regions where there is no luminous matter. Note the clustering in the open model appears very "tight"; substructure within clusters is generally not resolvable in the plots by the final epoch. The lack of significant initial power on large scales prohibits the growth of structures on 10 megaparsec scales in this model.

Comparison of the galactic distribution in the dark matter (DM) models, Figure 1, with that of the single particle galaxy (SP) runs, shown in Figure 2, illuminates an important difference between the clustering properties of the two representations. In the $\Omega_f = 0.15$ DM model, the large association in the lower right corner has not collapsed to form a single unit as has happened in the SP run. The same is true for the smaller grouping in the top center of the field in the $\Omega = 1.0$ models. It appears that the growth of some structures in the dark matter models has been suppressed or delayed relative to the point mass case. This must arise from the extended nature of the mass distribution in the DM runs. The smoothness introduced by the halos reduces peculiar accelerations on scales somewhat less than or comparable to the initial halo diameter. This will delay an initial phase of small-scale clustering. The process perpetuates to larger scales: the "seeds" formed at a given level of clustering in the DM runs may again be more extended than those formed at the same level in the SP case, slowing the clustering at this level, and so on.

More important differences between the two representations will show up on scales smaller than 20 Mpc. To exhibit these differences, the large cluster in the lower right corner is examined in greater detail in Figure 3. Complementary projections on two different scales, centered on the cluster core, are shown for each model. The upper panels (Figs. 3*a*, 3*d*, 3*g*, 3*j*) show roughly the whole cluster, the width of the window is 13.2 Mpc for $\Omega = 1.0$ and 3.2 Mpc for $\Omega_f = 0.15$. The second set of panels (Figs. 3*b*, 3*e*, 3*h*, 3*k*) are enlargments by a factor of 4 of the first set. On the larger scale, it appears that the mass distribution in the DM models is somewhat more extended than that in the SP runs. However, the distribution of *galaxies* is more highly concentrated in the dark matter models, as wit-

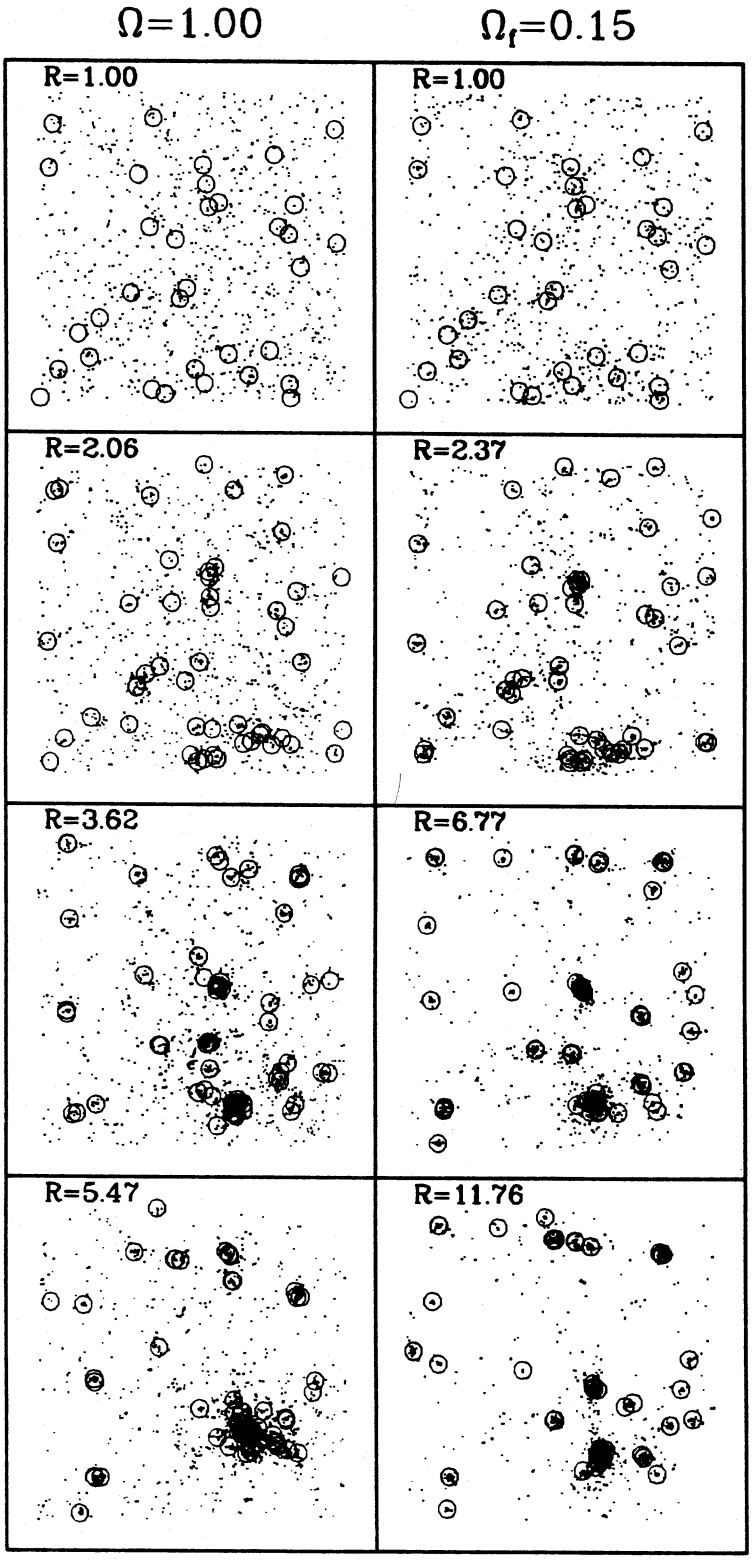

FIG. 1.—Projections on the *x-y* plane of the particle distributions in a 20 Mpc comoving cube of the dark matter (DM) models at different expansion factors. Luminous particles (galaxies) are plotted as circles, dark matter particles are plotted as points. The distribution of luminous matter is identical in both models initially. The larger halo radius in the $\Omega = 1.0$ model makes the halos appear as an almost smooth background. The large association in the lower right side is viewed in more detail in Fig. 3.

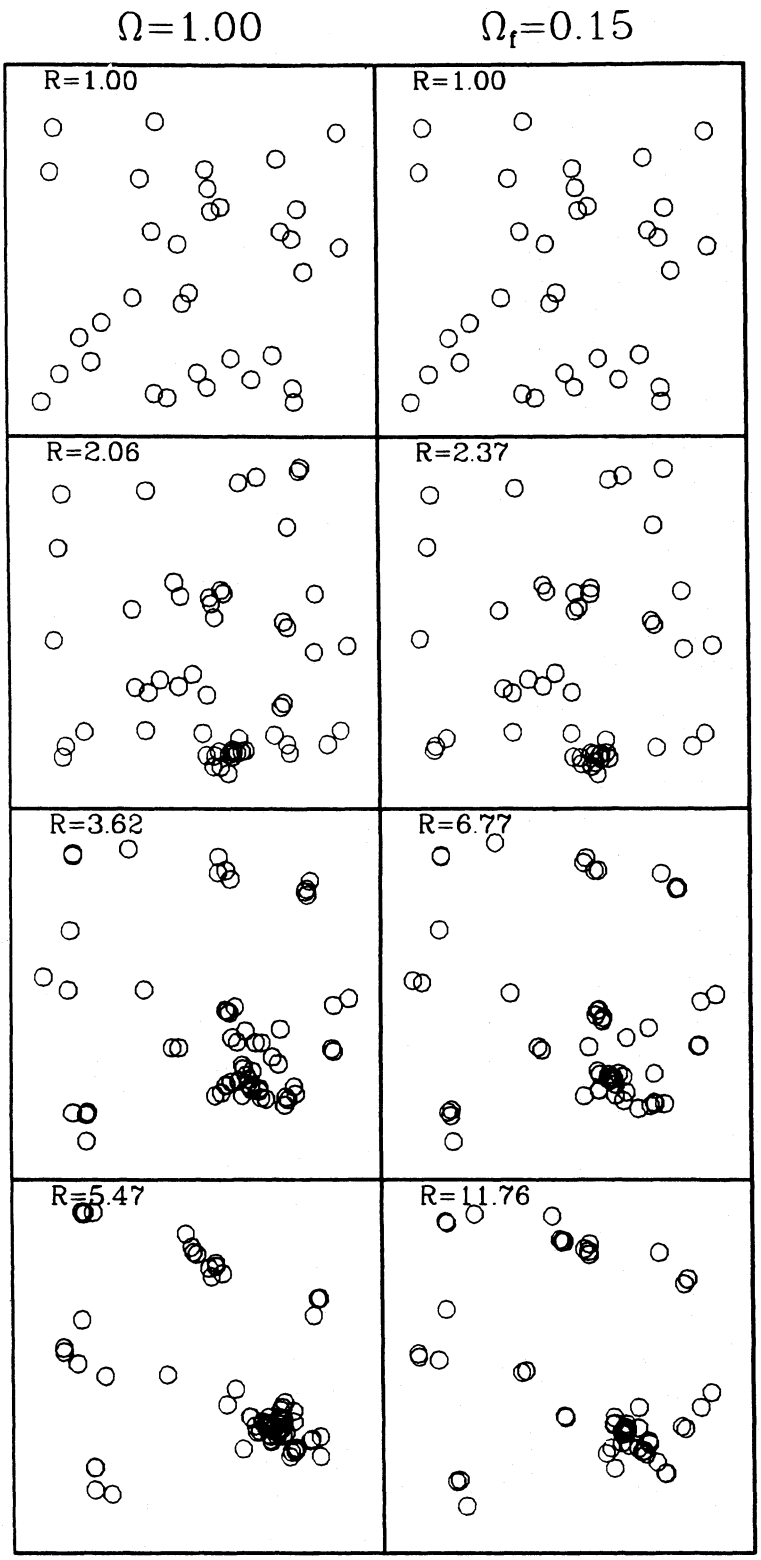

FIG. 2.—The same regions as in Fig. 1 are shown for the single particle (SP) representation. The stronger matter flows in these models allow collapse of structures not yet collapsed in Fig. 1, such as the lower right cluster in the $\Omega_f = 0.15$ model and the group in the upper center of the $\Omega = 1.0$ model.

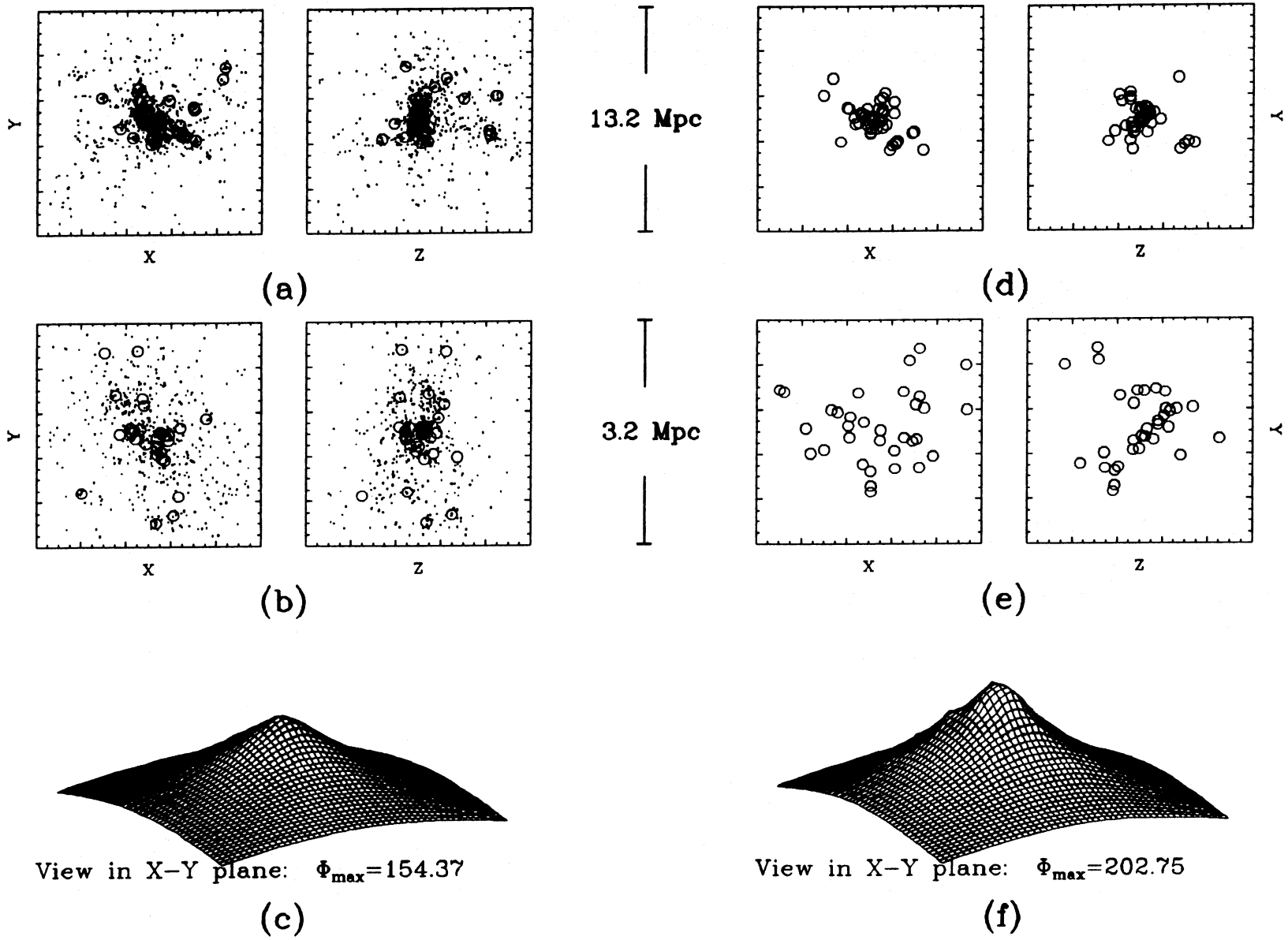

FIG. 3.—Close-up complimentary projections of the large clusters in the lower right of Figs. 1 and 2. (*a*) $\Omega = 1.0$ DM model; (*b*) same as (*a*) but enlarged by factor of 4; (*c*) two-dimensional potential $\phi = Gm \ln (r^2 + \epsilon^2)$ measured on a 50×50 grid superposed on projected mass distribution in *x*-*y* plane (*left panel of* [*a*]). Height of graph measures magnitude of potential at each grid point. (*d*–*f*) same as (*a*–*c*) but for $\Omega = 1.0$ SP model. (*g*–*l*) same as (*a*–*f*) but for $\Omega_f = 0.15$ DM model; note smaller window size.

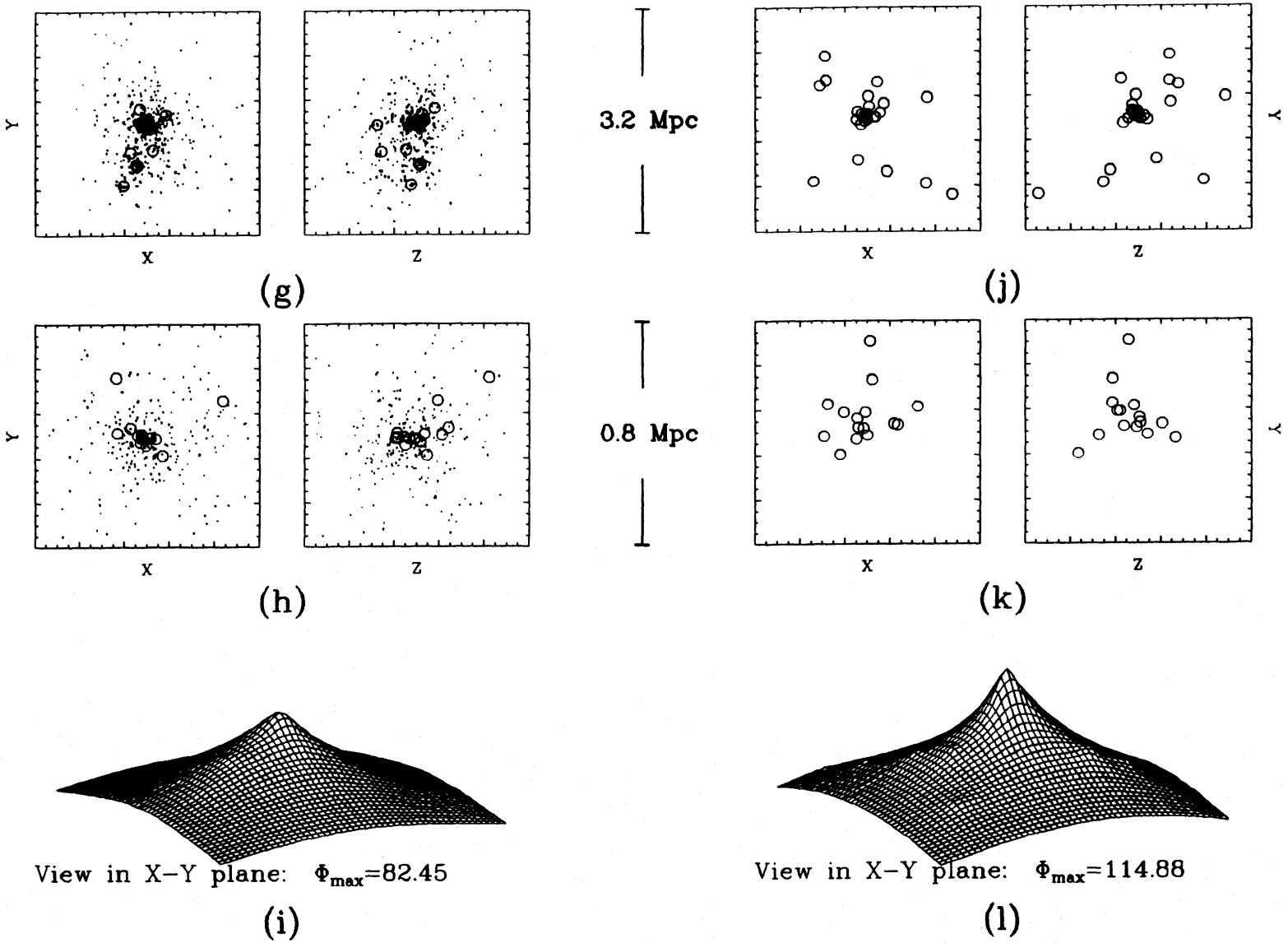

Fig. 3 *continued*

TABLE 2

CLUSTER GALACTIC CORE PROPERTIES

Model	r_{core} (Mpc)	$\delta\rho_{gal}/\rho_{gal}$	N_{gal}
$\Omega = 1.0$, DM	0.3	2×10^4	19
$\Omega = 1.0$, SP	1.0	1×10^3	30
$\Omega_f = 0.15$, DM	0.07	2×10^6	10
$\Omega_f = 0.15$, SP	0.2	9×10^4	14

nessed in the smaller scale projections. Table 2 lists estimates for the galactic core radius, core membership, and overdensity for the cluster in each model. The core is $\sim 50\%$ more massive in the single particle representations, but it is a factor of ~ 3 smaller in size and ~ 20 times as overdense in galaxies in the dark halo models. The cluster core in the dark matter models may be a good site for the formation of a dominant cD galaxy, especially in the open model where 10 galaxies are found within an inner 70 kpc radius. Studies by Merritt (1983) and Richstone and Malamuth (1983) have demonstrated the capacity for formation of a cD galaxy in clusters where dissipational encounters are explicitly included. Dynamical friction plays the important role of keeping velocities low while increasing the galactic density in central regions, thus allowing cannibalism to take place (Hausman and Ostriker 1978). The likelihood of cD formation should be larger in the open model for two reasons. First, the higher initial concentrations of dark matter around galaxies will improve the effectiveness of dynamical friction by increasing the local density of dark matter. Second, as we shall see below, the relative velocities of galaxies are appreciably smaller in the $\Omega_f = 0.15$ model than in flat universe.

To get an idea of the full kinematic distribution in the cluster, the *two-dimensional* potential, $\phi(r) = Gm \ln (r^2 + \epsilon^2)$, is measured on a grid laid down on the larger x-y projections shown in Figure 3 (left panels of 3*a*, 3*d*, 3*g*, 3*j*). The magnitude of the potential at each grid point is measured by the height of the three-dimensional plots shown in the bottom panels of Figure 3. The central potentials in the dark matter models are between 30% to 40% smaller than in the single particle representations, indicating that redistribution of mass plays an important part in reducing velocity dispersions in the former.

The general picture that emerges from visual inspection of the models is that the clustering in the DM models is more quiescent than that which develops when all mass is fixed to the galaxies. The halos serve to smooth the local potential which reduces forces, then act as shock absorbers, cushioning the fall of galactic systems into the local potential well. The heavier luminous population is eventually distilled to the bottom of the wells by dynamical friction. The comparatively hard single particle galaxies, on the other hand, create very "lumpy" potentials and have no "hidden" energy outlets available. They are therefore resigned to zip around the cluster in a manner dictated by the global cluster potential, which remains reasonably fixed in time. High central densities cannot be achieved because the central velocity dispersion is too high. The result is the massive but loose cluster cores observed in the SP runs as opposed to the lighter but more compact cores in the DM models.

b) *Two-Point Positional Correlations*

The lack of redshift-independent distance indicators for most galaxies precludes determination of their individual positions and velocities relative to the expanding background. The *relative* positions and motions random pairs of galaxies, however, provide a good deal of information on large-scale structure. The two-point correlation function has been measured extensively by Peebles and collaborators (Davis and Peebles 1983, and references therein) and others (e.g., Bean *et al.* 1983) to have the form

$$\xi(r) = (r/10 \text{ Mpc})^{-1.8} . \quad (8)$$

Gott and Turner (1979) analyzed a sample of closely spaced galaxy pairs in the Zwicky catalog and found the clustering from 10 to 50 kpc is consistent with that given in equation (8). The best fit of a power law to the small scale data alone yields a somewhat steeper slope, -2.1 rather than -1.8.

The data sample used for the two-point analyses consists of all pairs of luminous particles with separations $r \leq L/6 = 10.5$ Mpc in each model. Periodic boundary conditions are used to sample the volume completely. The total number of pairs is given in Table 3. Note the pair count within this cutoff expected from a random distribution of particles is 6206. All error bars in this section are determined by dividing the cubic simulation into octants—the mean and standard deviation of mean among the eight subvolumes determines the data value and error in each bin. This method is superior to simple "root N" statistics because the pairwise data are not independent; a cluster of N galaxies contributes $\sim N^2/2$ pairs, all of which are not independent. The uncertainties as measured here reflect the variations induced by sampling in different physical locations. Thus, they more accurately represent the "true" errors which may arise from dealing with a volume limited sample.

An evolutionary plot of the two-point correlation function, $\xi(r)$, measured in the proper frame is given in Figure 4. Error bars are plotted on the data at the final epoch only, uncertainties at other epochs are similar. The heavy solid line in Figure 4 is the observed correlation function, equation (8). At early epochs, $R = 2.0$ ($\Omega = 1.0$) and $R = 2.3$ ($\Omega_f = 0.15$), the weaker peculiar accelerations on scales $r \leq r_t$ are exhibited by the depressed values of $\xi(r)$ in the DM runs relative to their SP counterparts. On the larger scales, the representations are in agreement. On the smallest scales, evidence for enhancement of correlations due to dynamical friction is becoming apparent in the $\Omega_f = 0.15$ model. As groups and clusters evolve, the heavier luminous particles will sink to form a dense core embedded in the envelope of lighter particles (witness Fig. 3*h*). Thus, the disparity in the small-scale amplitude of $\xi(r)$ increases with time until, by the final epoch, the amplitude in the DM models is more than an order of magnitude greater than the SP runs. Note that the situation is not as dramatic for $\Omega = 1.0$, where $\xi(r)$ in the DM and SP runs differ appreciably on small scales only at the final epoch, $R = 5.4$. The lack of high dark matter concentrations around luminous particles intially in this case prevents dynamical friction from becoming important until structures have accreted enough material to raise the density to significant levels.

TABLE 3

COUNTS OF PAIRS WITH $r \leq 10.5$ Mpc

Ω_f	DM	SP
1.0.....	11402	14126
0.15.....	9507	10807

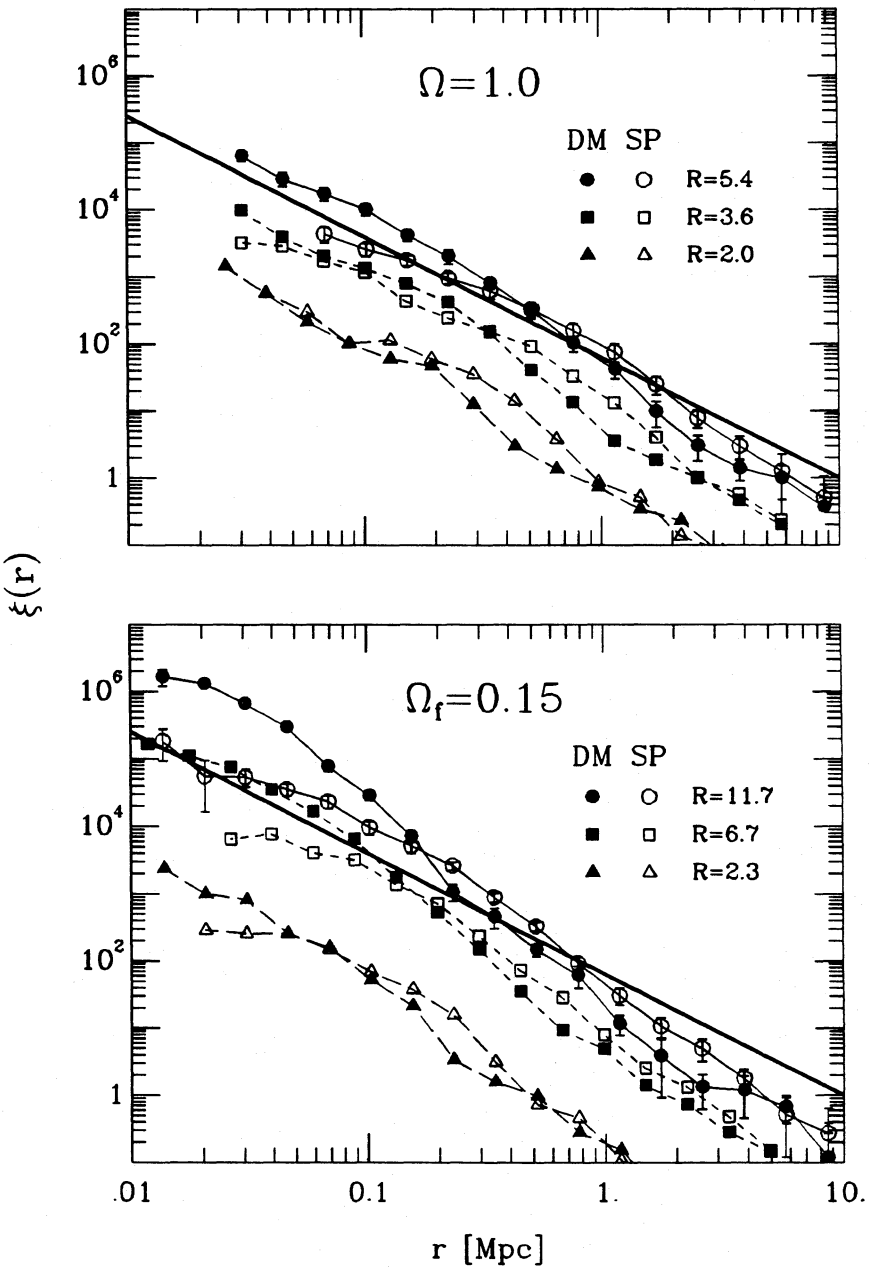

FIG. 4.—Evolutionary plot of the two-point correlation function $\xi(r)$. The solid line is the observed behavior, eq. (8).

The clustering suppressed by the weaker peculiar accelerations appears to persist throughout the evolution, bootstrapping its way up to larger scales, as is evident in Figure 4. This difference is illustrated more clearly by the statistic $J_3(r) = 4\pi n \int_0^r dx x^2 \xi(x)$, which measures the excess number of neighbors within a distance r of a given galaxy. Figure 5 shows $J_3(r)$ at the final epoch for each model. Weakened clustering is apparent on scales $r \geq 1$ Mpc in both cosmologies, neighbor counts being down by as much as 40%.

On scales where $\xi(r) \leq 1$, the correlation functions of the two representations agree within the uncertainties. In particular, the "correlation length" r_0, the separation at which $\xi(r) = 1$ is very similar for all four runs, $r_0 \approx 6$ Mpc for $\Omega = 1.0$ and $r_0 \approx 5$ Mpc for $\Omega_f = 0.15$. These values are smaller than the observed value because $\xi(r)$ is steeper than observed when white noise initial conditions are used.

At the final epoch, none of the models are able to reproduce the observed correlation function over the entire range shown in Figure 4. The clustering is significantly weaker on scales greater than a few Mpc and is stronger in the DM models on scales below $\sim$200 kpc ($\Omega_f = 0.15$) and $\sim$700 kpc ($\Omega = 1.0$). The large-scale problem will be helped by using initial conditions with more power on these scales. The small-scale discrepancy is much larger in the low-density model, which began with higher local densities of dark matter around galaxies and also was evolved for $\sim$16 billion yr compared to $\sim$11 billion yr for the flat model. Both of these factors serve to increase the effects of dynamical friction.

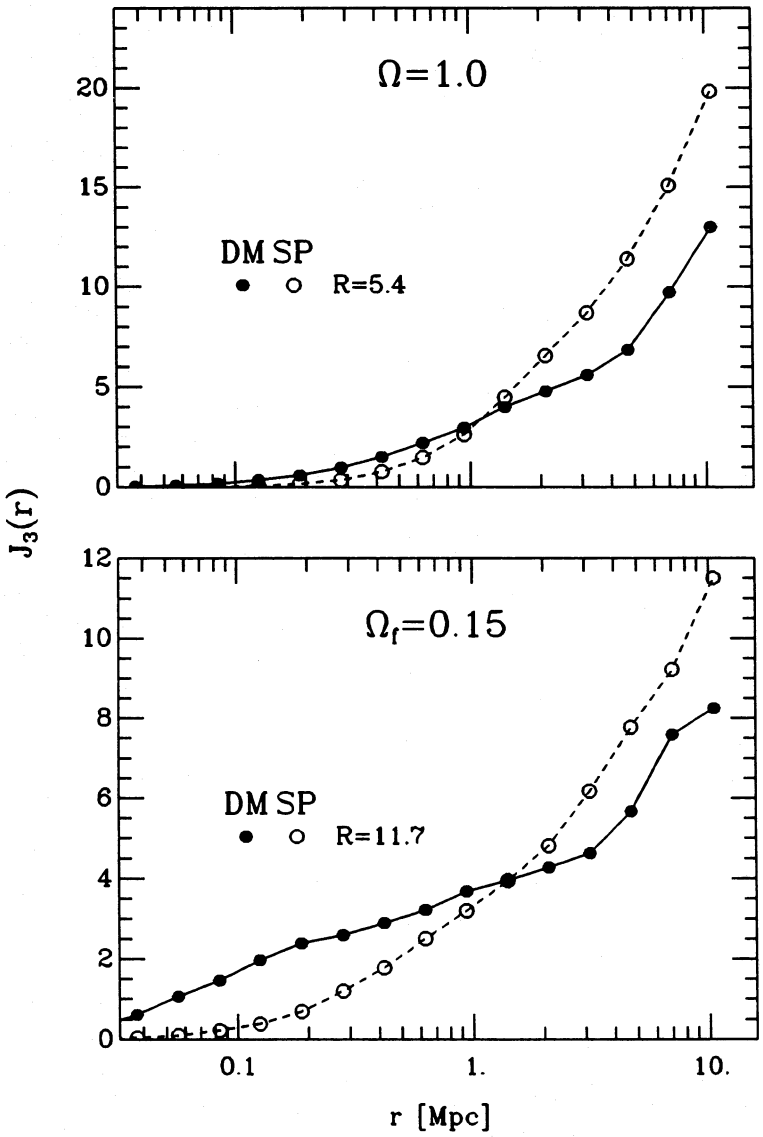

FIG. 5.—The excess neighbor count $J_3(r)$ at the final epoch. The weaker clustering in the DM models on scales $r > 1$ Mpc is more evident in this statistic than from the correlation function $\xi(r)$ in Fig. 4.

Galaxy mergers will provide a means of reducing the pair count at small separations. However, to produce agreement with observations in the low-density model, merging must be extremely efficient. The total number of pairs in this model with separations $r \leq 125$ kpc is 789, while that expected from the observed $\xi(r)$ is only 70. Simulations have shown that the luminous particles representing galaxies in this model will merge if their relative position and velocity satisfy this rough criterion (Roos and Norman 1979; Jones and Efstathiou 1979)

$$v(r) < 353[1 - r/(105 \text{ kpc})] \text{ km s}^{-1} . \quad (9)$$

This velocity should be compared to the three-dimensional velocity dispersion at small separations, which from Figure 6 below is $\sigma_{3d} = (3)^{1/2} \times 275$ km s^{-1} = 475 km s^{-1}. Assuming a Maxwellian velocity distribution, only 1.3% of pairs with separations $r = 50$ kpc will have velocities small enough for merger, $v < 177$ km s^{-1}. Even taking the maximum velocity at zero separation, one would expect only 9.3% of pairs to be merger candidates.

One should be cautious about rough calculations of this type. The merging condition, equation (9), was determined from collisions between two distinct, bound, and otherwise isolated objects, with well-defined half-mass radius. The conditions for merger of the luminous parts of two galaxies within individual or common dark halos may be much more complex. Indeed, the luminous matter in Barnes's (1985) small group simulations merged fairly rapidly. The half-*light* radius of a typical galaxy is small—a few tens of kpc or less—physical merger of the luminous parts of galaxies can only take place at separations comparable to this size. The enhancement of $\xi(r)$ in the low-density model kicks in on scales comparable to the halo size, 100–200 kpc. It is not clear how mergers on scales of 10 kpc would affect the number of pairs found at 100 kpc. Detailed collision simulations with galaxies in extended halos would be useful in shedding light on this situation.

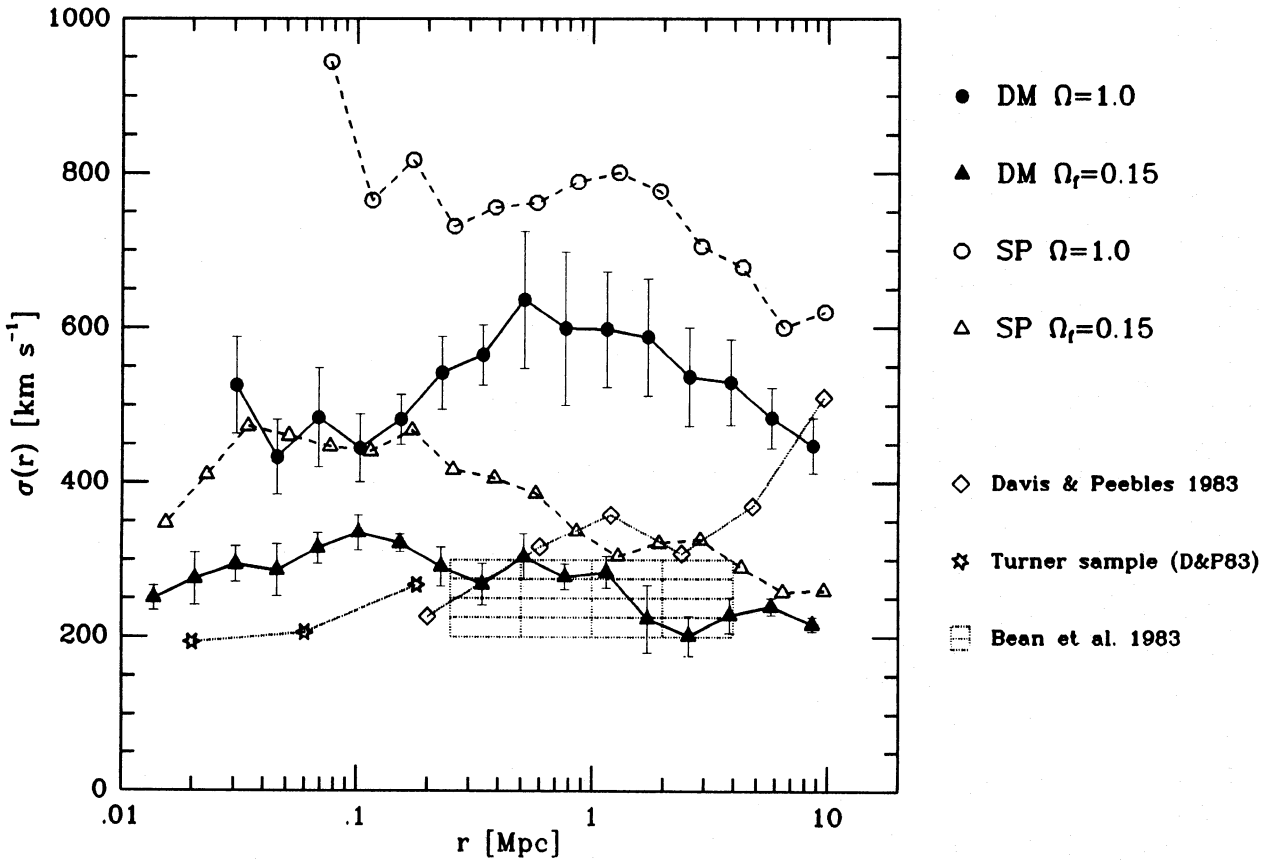

FIG. 6.—The rms one-dimensional velocity dispersion $\sigma(r)$ for pairs in the models at the final epoch. Filled circles: $\Omega = 1.0$ DM; open circles: $\Omega = 1.0$ SP; filled triangles: $\Omega_f = 0.15$ DM; open triangles: $\Omega_f = 0.15$ SP. Also shown are observational data—inverted triangles and hexagons: Davis and Peebles (1983); the boxed region is the data of Bean *et al.* (1983) who quote $\sigma(r) = 250 \pm 50$ km s^{-1} in the range indicated. Error bars on the SP are not shown, but are similar in magnitude to those on the DM data. Observational uncertainties are of order 50 km s^{-1}.

c) *Two-Point Velocity Correlations*

The relative peculiar velocity dispersion $\sigma(r)$ among galaxy pairs is not as well determined as the two-point positional correlation function $\xi(r)$. Davis and Peebles (1983) found $\sigma(r_p)$ to rise with separation in the CfA catalog, roughly following $\sigma(r_p) = 310(r_p/\text{Mpc})^{0.13}$ km s^{-1}. A similar analysis by Bean *et al.* (1983) on the Durham-AAT sample yielded results consistent with no trend in separation, $\sigma = 250 \pm 50$ km s^{-1} for 500 kpc $\leq r_p \leq 4$ Mpc. A different approach by Rivolo and Yahil (1981) with the RSA sample also produced results independent of r_p but with much lower magnitude, $\sigma = 100 \pm 15$ km s^{-1}. Even with the observational uncertainties, the velocity dispersion $\sigma(r)$ remains a useful comparitor for cosmological models, since values of $\sigma \geq 400$ km s^{-1} for $r \leq 5$ Mpc are ruled out by all the observations.

The rms one-dimensional velocities of galaxy pairs as a function of full three-dimensional pair separation are shown in Figure 6 along with some of the observations quoted above. Note the observed values are rms line-of-sight velocities versus projected separation. This comparison is valid if contamination from "accidental" pairs (i.e., pairs associated in projection, but not in three dimensions) is small, for projection of a physically associated pair will not smear its signal out widely on the log r axis used in Figure 6. Again, error bars are determined from sampling individual octants within the simulation cube. Velocities in the DM models are significantly lowered relative to the SP case. The $\Omega_f = 0.15$ DM model exhibits the best agreement with observations for separations $r \leq 1$ Mpc, where $\sigma \approx 300 \pm 50$ km s^{-1} independent of separation within the errors. At larger separations, σ falls slightly, as do velocities in all the runs beyond $r \approx 1$ Mpc. The small-scale velocity in the open SP model is $\sigma \approx 450$ km s^{-1}, 50% larger than the DM run and significantly higher than observational values. The flat DM velocities increase with separation from $\sigma \approx 450$ km s^{-1} at $r \approx 100$ kpc to $\sigma \approx 600$ km s^{-1} at $r \approx 500$ kpc, then decline slowly back to $\sim$450 km s^{-1} at $\sim$10 Mpc. The $\Omega = 1.0$ SP model, as expected, generates very large velocities on small scales: $\sigma \geq 750$ km s^{-1} for $r \leq 1$ Mpc. The reduction in peculiar velocity in the dark matter models results from the combination of effects mentioned previously: smaller peculiar accelerations arising from the more extended mass distribution, the inelasticity of halo-halo interactions, and finally local effects of dynamical friction. It is difficult to delineate between these effects, but the combination results in a drop of pair kinetic energy per unit mass by a factor of $\sim 1.5^2 \approx 2.25$ on small scales relative to the softened point mass case.

An interesting feature shows up in the mean radial *proper* velocity of pairs shown in Figure 7. The $\Omega_f = 0.15$ dark matter model shows strong radial inflows of up to 200 km s^{-1} between 1 and 2 Mpc where none are evident in the SP case. Collapse in the latter run is evidently complete and clusters on the average are "virialized"—neither expanding nor contracting. The streaming in the DM run may be the signature of the

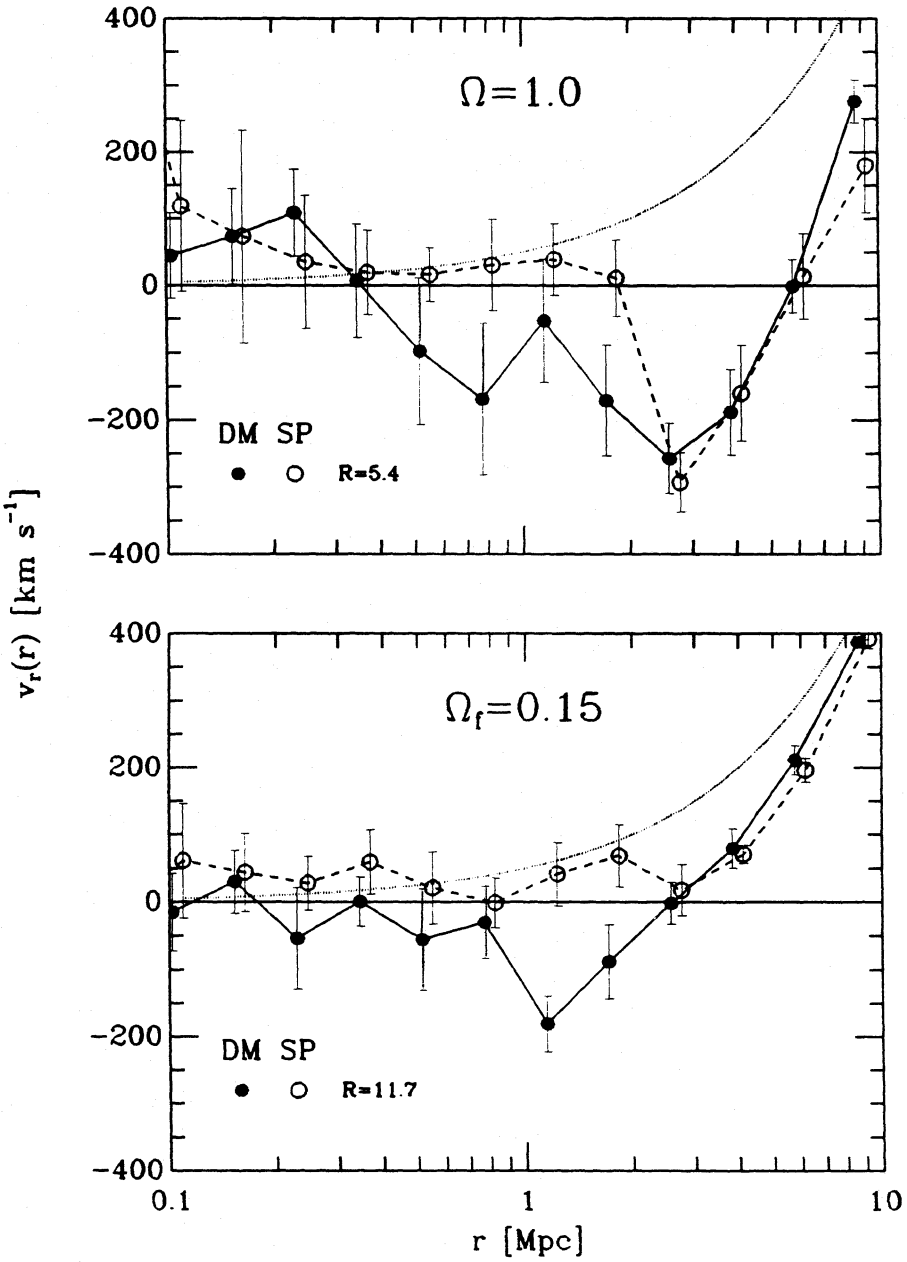

FIG. 7.—The mean radial proper velocity v_r vs. separation for the models at the final epoch. The DM models exhibit inflows in regions where none are seen in the SP representation. The thin line is the Hubble relation, $v_r = H_0 r$.

collapse of systems delayed relative to the SP case. More likely, it is a sign of the inelastic processes at work in the outer regions of groups and clusters. Galaxies at larger radii are having their halos sheared off and added to the cluster background. They then are drawn to the group center by dynamical friction. The result is a net "inflow" of galaxies to smaller separations. Similar evidence of this secular evolution is seen in the $\Omega = 1.0$ model between 0.5 and 2 Mpc, although the scatter among pairs is much larger. Beyond 2 Mpc, infall is seen in both matter representations as structures continue to collapse on these scales.

d) Binaries

The sample of isolated pairs of galaxies (binaries) is defined here to be those pairs whose members are each others' nearest neighbors. In terms of a simple isolation parameter for pair ij

$$y_{ij} = \min \frac{(r_{ik}, r_{jk})}{r_{ij}}, \qquad (10)$$

where k runs over neighbors of the pair, pair ij is a binary if $y_{ij} > 1$. Observational definitions of binaries using projected separations in equation (10) have generally been more stringent, for example, $y > 3$, to at least partially compensate for uncertainties introduced by projection effects.

The kinematics of binaries represent an important link in the chain of reasoning which demonstrates the existence of massive dark halos around galaxies out to distances approaching 1 Mpc (see references cited in § I). The independence of binaries' relative velocities as a function of separation is indirect evi-

dence for the existence of such halos, but mass estimates are hampered by small samples and uncertainties in orbital parameters such as eccentricity. Nevertheless, the Keplerian behavior of binary velocities found by Evrard and Yahil (1985) in the N-body models of Efstathiou and Eastwood (1981) indicates that binary dynamics are not well modeled by the interaction of pairs of softened point masses.

The evolution of isolated pair counts is shown in Figure 8, where the number of binaries is plotted against separation at three epochs. Figure 9 shows the one-dimensional rms velocity of binaries as a function of separation at the final epoch only, along with the observational results of White *et al.* (1983) and Peterson (1979). The strong effects of dynamical friction are apparent again in the dark halo models, and again, more so in the low-density model. With single particle galaxies, the pair count distribution does not significantly evolve with time, apart from those binaries with wide enough separations to be unbound.

In contrast, binaries in the DM models evolve systematically toward smaller separations as the heavy galaxies spiral to the center of their common halo. An example binary is shown in Figure 10, where the particle distributions at an early epoch, $R = 2.0$ for $\Omega = 1.0$ and $R = 2.3$ for $\Omega_f = 0.15$, and at the final epoch are shown. The size of the window shown in the figures is the same at both epochs but differs between the cosmologies, being 2 Mpc for the flat model and 1 Mpc for the open. Individual galactic halos are evident at the early time when the galaxies are separated by ~ 1.2 Mpc ($\Omega = 1.0$) and ~ 450 kpc ($\Omega_f = 0.15$). By the final epoch, the halos have merged and the galaxies are now separated by only 160 kpc and 45 kpc, respectively. This "distillation" process is so efficient in the open model that the binary distribution in Figure 8 becomes virtually bimodal: evolved systems lie in the range $r \leq 80$ kpc, unbound and expanding pairs have separations $r \geq 1$ Mpc, and a rather empty region exists between. Of the 187 binaries with separations $r \leq 1$ Mpc, 169 lie below 80 kpc, leaving only 18 in the range $80 \leq r/\mathrm{kpc} \leq 1000$. This conflicts with observational data, such as the Turner sample, where roughly one third (25 out of 73) of the pairs in the culled sample defined by White *et al.* (1983) have projected separations $r_p \geq 80$ kpc. If one believes that the mass and size of the halos in the open model are realistic, one is led to the conclusion that real binaries must be much younger than these simulated systems. The same conclusion was reached by Barnes (1984) in his study of small groups which also had 90% of the total mass initially in extended halos around galaxies.

The velocities in the $\Omega_f = 0.15$ DM model shown in Figure 9 again show better agreement with the observational data than do any of the other runs. The point mass models exhibit essentially Keplerian behavior, $v \propto r^{-1/2}$. The $\Omega = 1.0$ DM velocities are consistent with flat at $v(r) \approx 300$ km s^{-1} over about a decade in separation between 100 kpc and 1 Mpc. Velocities below 100 kpc rise in a nearly Keplerian fashion. This trait is not exhibited at earlier epochs and may be transient or may be an artifact of the coarse nature of the DM representation in this model: stripped galaxies may be interacting directly at these separations.

Binaries represent a significant fraction of the pair count at small separations. If merging were efficient enough in the low-density model to bring $\xi(r)$ into agreement with observation,

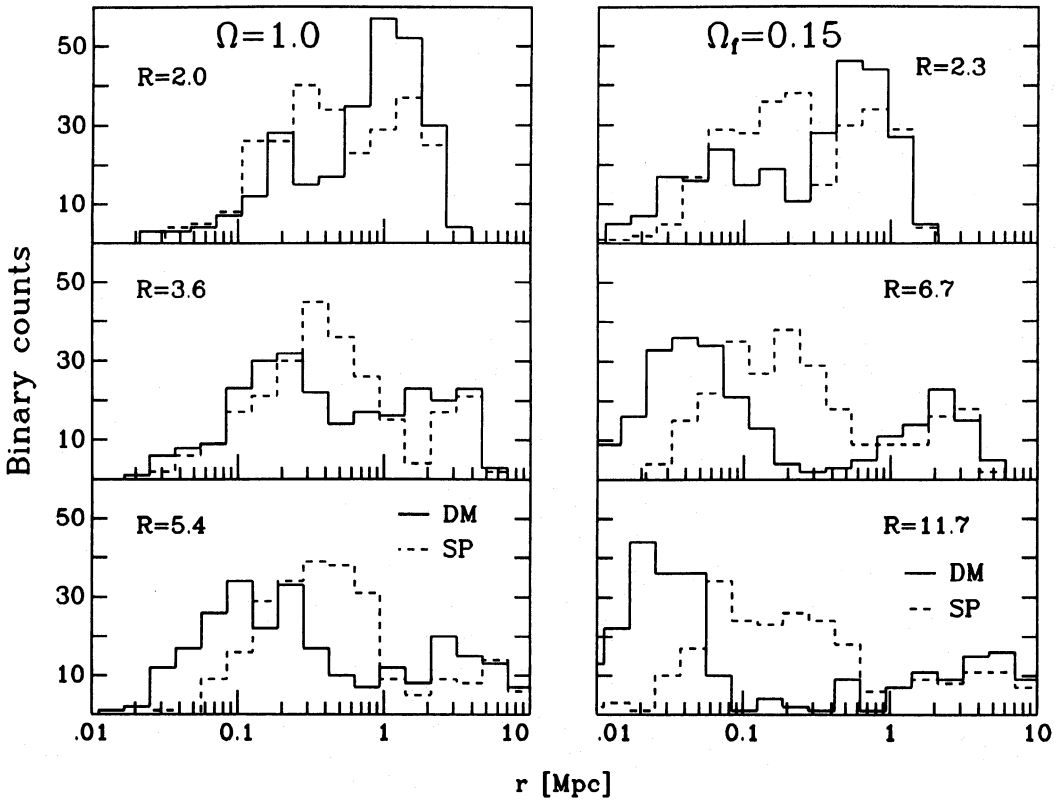

FIG. 8.—Counts of binaries at different epochs in the models. Solid histograms are data for the DM runs, dashed histograms for the SP models. Binaries in the former evolve in a secular fashion toward smaller radii. Note the "void" in the $\Omega_f = 0.15$ DM model between 80 kpc and 1 Mpc.

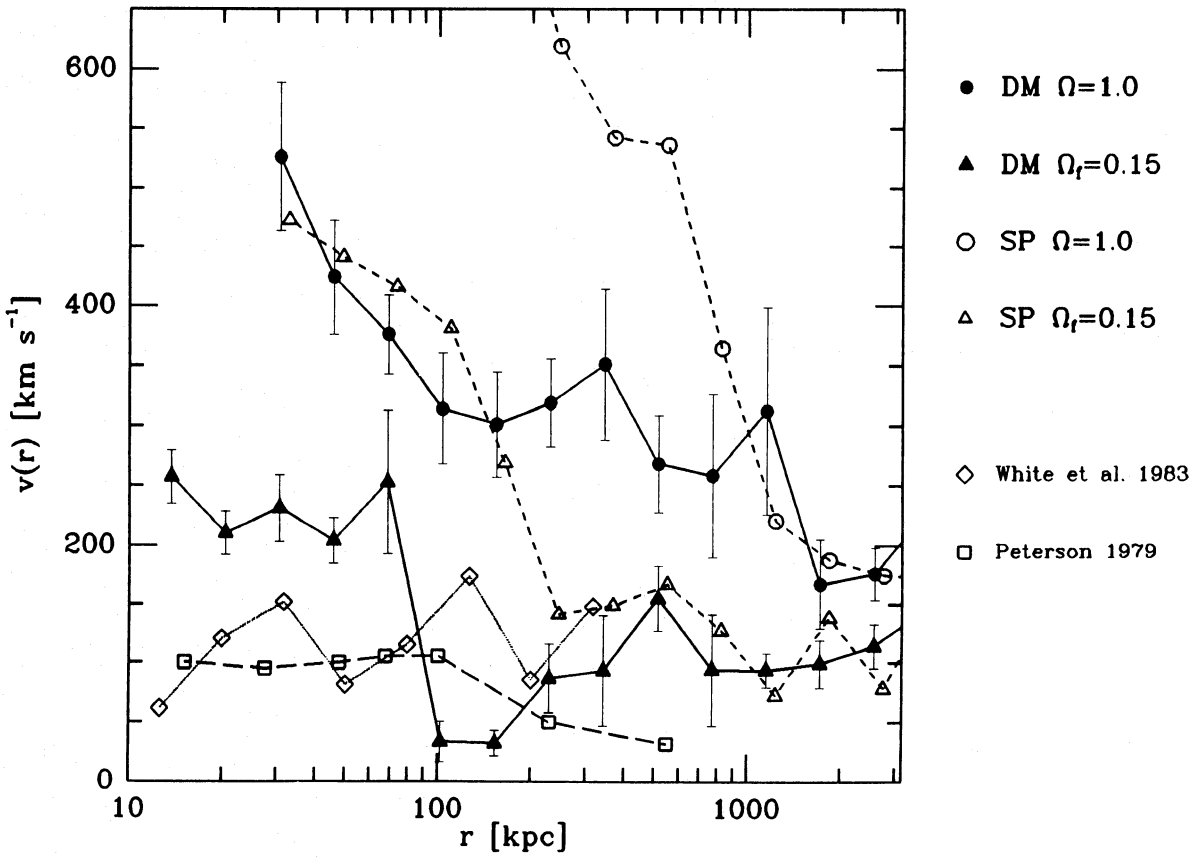

FIG. 9.—The rms one-dimensional velocities of binaries at the final epoch. Filled circles: $\Omega = 1.0$ DM; open circles: $\Omega = 1.0$ SP; filled triangles: $\Omega_f = 0.15$ DM; open triangles: $\Omega_f = 0.15$ SP. Also shown are observational data—inverted triangles: White *et al.* (1983); open squares: Peterson (1979).

then nearly all the small r binaries in this sample would have been merged. Of course, new binaries would be produced from among the merged population. However, if most binary members were merger remnants, it may be difficult to reconcile with the fact that the majority of observed binary systems consist of spiral-spiral pairs.

IV. DISCUSSION

The models presented in this paper represent a first attempt at simulating the large-scale clustering of galaxies possessing massive dark halos. The models are crude in some respects: only 25 particles per halo can be accommodated and a white noise initial fluctuation spectrum, utilized for computational economy, produces a two-point correlation function which poorly matches the observed power-law behavior. On the other hand, the inferred existence of extended dark matter halos around galaxies coupled with knowledge of the highly inelastic nature of halo-halo encounters obviates the need for simulations with a more realistic treatment of small-scale dynamics than that afforded by the softened point mass approach used in the past. Present technology force these limitations upon us.

The 25 particles in the halo increase the total number of degrees of freedom per galaxy from 6 to 156, and these essentially "hidden" degrees of freedom act as a sink into which energy accumulated in bulk motion can be diverted. Further, the extended nature of the mass distribution in the dark matter models reduces local peculiar accelerations. The most significant observable effects that arise are the lowering of galaxy pair peculiar velocities, particularly on scales $r < 500$ kpc, the enhancement of small-scale clustering through dynamical friction, and the suppression or delay of clustering on 1–5 Mpc scales. Binary velocities are also flattened by the addition of dark matter halos, but the distribution of binaries evolves significantly in the low density model to the point where almost no binaries are observed in the range $80 < r/\mathrm{kpc} < 1000$.

These effects are dependent on the model parameters chosen, most important of which are (1) the fraction of mass in the dark component f_d; (2) the ratio of halo size to initial intergalactic spacing, $\alpha = r_t/d_i$ (eq. [4]); (3) the ratio of species' particle masses, $\beta \equiv m_{\mathrm{dark}}/m_{\mathrm{lum}}$; and (4) the starting epoch $z_i = R_f - 1$. It is, of course, impractical to attempt to explore the above parameter space in extensive detail. One must, instead, rely on a mixture of physical intuition, (usually) vague dimensional arguments, and some trial and error. The amount of matter contained within the luminous parts of galaxies is thought to be small, $\Omega_{\mathrm{gal}} < 0.02$ (Yang *et al.* 1984). Thus, a choice of 90% of matter outside the luminous parts of galaxies is consistent with $\Omega_{\mathrm{tot}} = 0.15$ and may be conservative for $\Omega_{\mathrm{tot}} = 1.0$. Constraints on the parameter α would come from extending observed rotation curves out to larger radii or an improved dynamical analysis of binary galaxies. Numerical limitations control the range of β available in practice. If one believes the dark matter distribution around galaxies is lumpy with characteristic lump mass m_{dark}, then the model is realistic as it stand. Ideally, one would like to lower β by using $\sim 10^3$ particles per halo to better represent a smooth matter distribution. Unfortunately, this is not possible for large numbers of

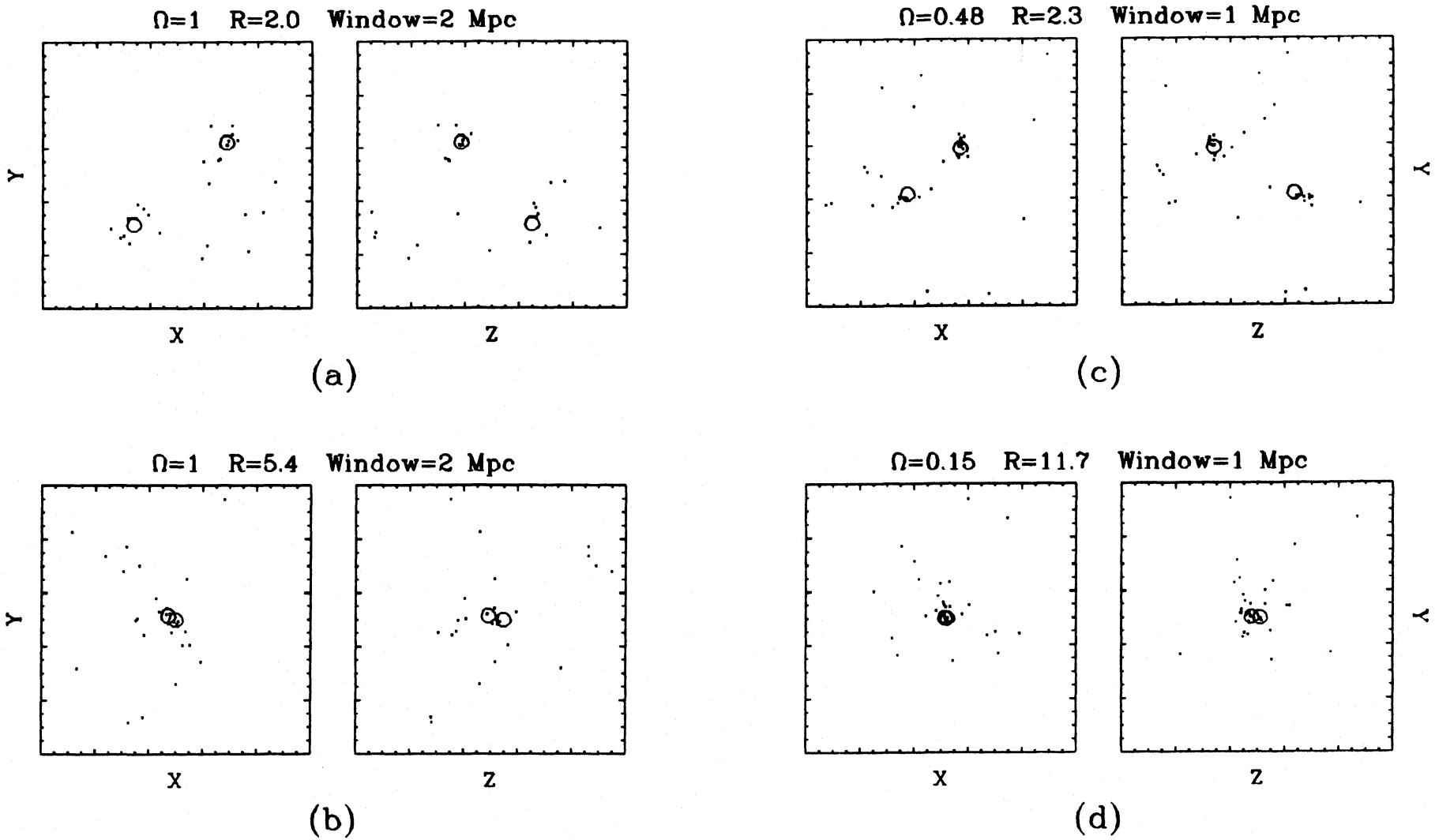

FIG. 10.—Complimentary projections of a binary system at two epochs in the DM models. The galaxies are circles and dark particles are points. The same binary is examined for both values of Ω. The window size is the same at each epoch but differs between cosmologies. Individual halos evident in the early frames, (*a*) and (*c*), merge to a common envelope by the final epoch, (*b*) and (*d*), while the separation between the galaxies shrinks by about a factor of 10.

galaxies with current methods. Finally, using an initial fluctuation spectrum capable of producing a power-law correlation function over a wide range of scales would eliminate the freedom in choosing R_f, as one would evolve the system until $\xi(r)$ matched observations.

One of the driving forces motivating simulations of large-scale structure is the determination of the density parameter of the universe, Ω_0. The important question is whether Ω_0 is equal to one or not. The $\Omega_f = 0.15$ model is attractive for its low velocities, which are in good agreement with observations. The effects of dynamical friction, however, are quite strong with the parameters chosen in this model. The enhancement of $\xi(r)$ on small scales is not consistent with observations. Only one measurement of $\xi(r)$ has been done on very small scales with a sample containing only 47 pairs of galaxies (Gott and Turner 1979). The data do show a tendency toward enhanced clustering below 50 kpc, but poor statistics make it impossible to distinguish significant differences between the small- and large-scale behaviors of $\xi(r)$. An improved measurement of the correlation function at small scales is important to resolving this issue. Note the small-scale effects on $\xi(r)$ are much weaker in the $\Omega = 1.0$ model which differs from the $\Omega_f = 0.15$ model in having a smoother initial dark matter distribution (larger α) and being evolved for a shorter period of time. By adjusting the available parameters, the effects on $\xi(r)$ at small scales may be minimized.

The scaling method used in § II to determine r_t yielded a value of $\alpha = 1.6$ for the $\Omega = 1.0$ model, indicating extensive overlap of galactic halos initially. This conflicts with the simple physical picture one would like to envision where distinct halos form first, creating the potential wells into which gas can cool and form galaxies. This picture works very well in the low-density case, where $\alpha = 0.6$ implies the halos are just touching initially. Attempting to use this value of α in the flat model would imply a rotation velocity $v_{\rm rot} \approx 330$ km s^{-1}, a value considerably higher than any yet observed (Bahcall and Casertano 1985). Alternatively, the 200 km s^{-1} halos truncated at $r_t = 2.1$ Mpc used in this model will be volume filling at a redshift $z = 1.06$. *It is therefore difficult to envision as realistic an* $\Omega = 1.0$ *universe in which bright galaxies with extended massive dark halos contain all the mass.* An obvious way around this is to put mass where there are no galaxies. Biased galaxy formation (Kaiser 1984; Bardeen 1986) provides a prescription for selecting regions of galaxy formation based on a local density criterion. This or some other biasing mechanisms will serve to reduce the mass per galactic system, allowing smaller halos for a given $v_{\rm rot}$. It will also decrease the amount of mass in the local neighborhood of galaxies, reducing small-scale galactic peculiar velocities, possibly enough to being them into line with observations. The good agreement of the $\Omega_f = 0.15$ DM velocities with observations suggests that the proper amount of biasing in an $\Omega = 1.0$ model should select $\sim 15\%$ of the total mass to be in the local neighborhood of galaxies. Although biasing may allow an $\Omega = 1.0$ cosmology to masquerade as a low-density model on small scales, differences should be apparent on larger scales, where bulk matter currents should be considerably larger in the former due to the gravitation of the unseen mass between groups and clusters of galaxies. Preliminary results announced by Faber (1986) and her collaborators indicate that substantial large-scale flows, $v \approx 500$–600 km s^{-1}, may exist on the largest observed scales, 50 to 100 Mpc. Such large-scale currents may be difficult to produce in a low-density model without resorting to extreme amounts of power in the initial fluctuation spectrum on these scales. A properly biased $\Omega = 1.0$ model may be capable of producing such large-scale flows while retaining small-scale velocities in agreement with observations.

This work constitutes part of a doctoral thesis performed at SUNY–Stony Brook. Much of the work in this paper was done while visiting at the Institute of Astronomy, Cambridge University. It is a pleasure to thank my thesis advisor, A. Yahil, for helpful criticism and several important contributions, particularly for suggesting the use of nonequilibrium isothermal profiles for the initial halos. I am indebted to G. Efstathiou and collaborators—S. White, M. Davis, and C. Frenk—for use of the P^3M code, without which this work would have been impossible. The author benefitted from discussions with many co-workers while visiting the IOA, among them G. Efstathiou, B. Saslaw, N. Kaiser, and S. Aarseth. I am grateful to the IAO for its hospitality and for the use of computer resources. This work was funded by USDDW grant DE-AC02-80ER10719 at the State University of New York.

REFERENCES

Alladin, S., and Narasimhan, K. 1983, *Phys. Repts.*, **92**, 339.
Bahcall, J. N., and Casertano, S. 1985, *Ap. J. (Letters)*, **293**, L7.
Bardeen, J. M. 1986, in *Inner Space/Outer Space*, ed. E. W. Kolb *et al.* (Chicago: University of Chicago Press), p. 212.
Barnes, J. 1983, *M.N.R.A.S.*, **203**, 223.
———. 1984, *M.N.R.A.S.*, **208**, 885.
———. 1985, preprint.
Bean, A. J., Efstathiou, G., Ellis, R. S., Peterson, B. A., and Shanks, T. 1983, *M.N.R.A.S.*, **204**, 615.
Davis, M., Efstathiou, G., Frenk, C. S., and White, S. D. M. 1985, *Ap. J.*, **292**, 371.
Davis, M., and Huchra, J. 1982, *Ap. J.*, **254**, 437.
Davis, M., and Peebles, P. J. E. 1983, *Ap. J.*, **267**, 465.
Des Forêts, G., Dominguez-Tenreiro, R. Gerbal, D., Mathez, G., Mazure, A., and Salvador-Solé, E. 1984, *Ap. J.*, **280**, 15.
Efstathiou, G., Davis, M., Frenck, C. S., and White, S. D. M. 1985, *Ap. J. Suppl.*, **57**, 241.
Efstathiou, G., and Eastwood, J. W. 1981, *M.N.R.A.S.*, **194**, 503.
Einasto, J., Kaasik, A., and Saar, E. 1974, *Nature*, **250**, 309.
Evrard, A. E. 1986, in preparation.
Evrard, A. E., and Yahil, A. 1985, *Ap. J.*, **296**, 299.
Faber, S. 1986, *Heineman Prize Lecture*, "*Galaxies and the Universe*," presented at 167th meeting of AAS, Houston, Texas.
Faber, S., and Gallagher, J. 1979, *Ann. Rev. Astr. Ap.*, **17**, 135.
Fabricant, D., and Gorenstein, P. 1983, *Ap. J.*, **267**, 535.
Geller, M., and Huchra, J. 1983, *Ap. J. Suppl.*, **52**, 61.
Gott, J. R., and Turner, E. L. 1979, *Ap. J. (Letters)*, **232**, L79.
Gott, J. R., Turner, E. L., and Aarseth, S. J. 1979, *Ap. J.*, **234**, 13.
Hausman, and Ostriker, J. P. 1978, *Ap. J.*, **224**, 320.
Heisler, J., Tremaine, S., and Bahcall, J. N. 1985, *Ap. J.*, **298**, 8.
Hockney, R. W., and Eastwood, J. W. 1981, *Computer Simulation Using Particles* (New York: McGraw-Hill).
Holmberg, E. 1941, *Ap. J.*, **94**, 385.
Jones, C., and Efstathiou, G. 1979, *M.N.R.A.S.D.*, 1983, **189**, 27.
Kaiser, N. 1984, *Ap. J. (Letters)*, **284**, L9.
Merritt, D. 1983, *Ap. J.*, **264**, 24.
Ostriker, J. P., Peebles, P. J. E., and Yahil, A. 1974, *Ap. J. (Letters)*, **193**, L1.
Peebles, P. J. E. 1980, *The Large-Scale Structure of the Universe* (Princeton: Princeton University Press).
Peterson, S. D. 1979, *Ap. J.*, **232**, 20.
Richstone, D., and Malamuth, E. 1983, *Ap. J.*, **268**, 30.
Rivolo, A. R., and Yahil, A. 1981, *Ap. J.*, **251**, 477.
Roos, N., and Norman, C. A. 1979, *Astr. Ap.*, **76**, 75.
Sandage, A., and Tammann, G. A. 1980, *Revised Shapley-Ames Catalog* (*Washington: Carnegie Institution of Washington*).
Sharp, N. A. 1984, *Ap. J.*, **286**, 437.

Stewart, P., Canizares, C. Fabian, A., and Nulsen, P. 1984, *Ap. J.*, **278**, 536.
Tremaine, S. 1981, in *The Structure and Evolution of Normal Galaxies*, ed. S. M. Fall and D. Lynden-Bell (Cambridge: Cambridge University Press), p. 67.
Van Albalda, T. S., Bahcall, J. N., Begeman, K., and Sanscisi, R. 1985, *Ap. J.*, **295**, 305.
White, S. D. M. 1978, *M.N.R.A.S.*, **184**, 185.
———. 1983, in *IAU Symposium 100, Internal Kinematics and Dynamics of Galaxies*, ed. E. Athanassoula (Dordrecht: Reidel), p. 337.
White, S. D. M., Huchra, J., Latham, D., and Davis, M. 1983, *M.N.R.A.S.*, **203**, 701.
White, S. D. M., and Rees, M. J. 1978, *M.N.R.A.S.*, **183**, 341.
Yahil, A. 1985, private communication.
Yahil, A., Sandage, A., and Tammann, G. A. 1980, *Ap. J.*, **242**, 448.
Yang, J., Turner, M. S., Steigman, G., Schramm, D. N., and Olive, K. A. 1984, *Ap. J.*, **241**, 493.

AUGUST E. EVRARD: Institute of Astronomy, Madingley Road, Cambridge CB3 0HA, England, UK